

I.F. OTHER MODES OF TRANSMISSION ELECTRON MICROSCOPE OPERATION

In addition to conventional bright field microscopy, the transmission electron microscope is capable of performing a variety of other useful functions, thus expanding the flexibility with which specimens may be critically examined. Some of the more common uses of the TEM, aside from bright-field operation, include:

Electron Diffraction
Dark Field Microscopy
High Resolution Microscopy
Tilting and Stereo Microscopy
Low Temperature Microscopy
Energy Loss Spectroscopy
X-ray Microanalysis

I.F.1. Electron Diffraction

Electron diffraction provides a basis for studying the structure of crystals and of identifying materials. Metals tend to give very strong electron diffraction patterns, whereas biological specimens generally diffract quite weakly.

a. Bragg's law

A crystalline specimen will diffract the electron beam strongly through well-defined directions (given in angles, θ) dependent on electron wavelength and crystal lattice spacing according to Bragg's law,

$$n\lambda = 2d \sin \theta$$

where n = integer

λ = electron wavelength

d = crystal lattice spacing between atomic planes

θ = angle of incidence and also of reflection

This relation gives the conditions for constructive interference of the scattered electron waves (Fig. I.152). There is reinforcement of reflections from successive parallel planes when the angles of incidence and reflection satisfy Bragg's Law. The spacing of spots (*i.e.* distance between spots) is reciprocally related to the lattice dimensions in the specimen. For example, with 100 kV electrons, ($\lambda = 0.0037$ nm) and a d -spacing for a typical biological crystal = 10 nm, $\sin \theta = 0.000185$ and the Bragg angle $\theta = 0.0106^\circ$. A typical d -spacing for a metallic crystal such as nickel is 0.203 nm, so $\sin \theta = 0.00911$ and $\theta = 0.522^\circ$. Note how the smaller d -spacing in the metal compared to a biological crystal leads to a larger scattering angle.

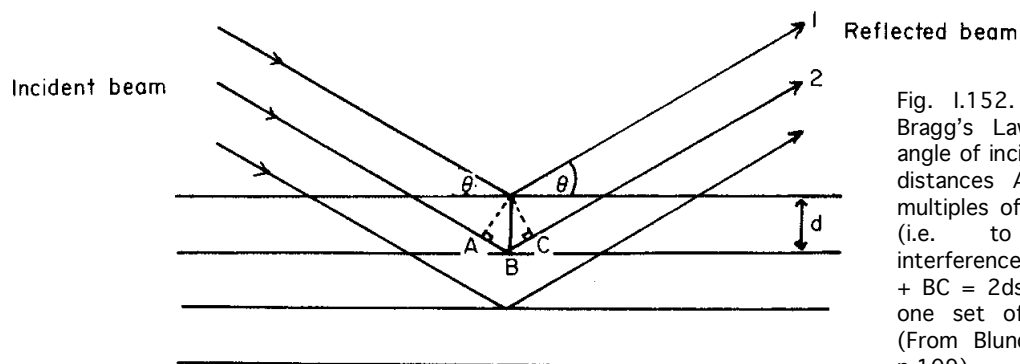


Fig. I.152. Bragg's Law. Here Bragg's Law is obeyed when the angle of incidence, θ , is such that the distances AB and BC are integral multiples of the electron wavelength (*i.e.* to give constructive interference). Note: the distance $AB + BC = 2d \sin \theta$. d is the spacing of one set of planes in the crystal. (From Blundell and Johnson, 1976, p.109)

Depending on the nature of the specimen, a diffraction pattern usually consists of a series of rings (for specimens consisting of many randomly oriented micro crystals) or a discrete lattice of sharp spots (for specimens with a single, crystalline domain). Each sharp spot (often called “Bragg reflection”) in the diffraction pattern from a crystalline specimen is an image of the electron source because the imaging system is set to put the image of the electron source onto the viewing screen when the microscope is operated in electron diffraction mode.

b. Camera length and camera constant

The camera constant is defined as λL , where L is the camera length (usually expressed in mm; typically $L = 300$ mm.) as shown in Fig. I.153. When the camera constant is known, the d spacings in the crystal can be calculated when R is measured. Note that, as the accelerating voltage is decreased (and electron wavelength, λ , increases), the scale of the diffraction pattern increases and the ED pattern expands. Hence, if voltage is increased, the scale of the ED pattern decreases and the pattern shrinks in size.

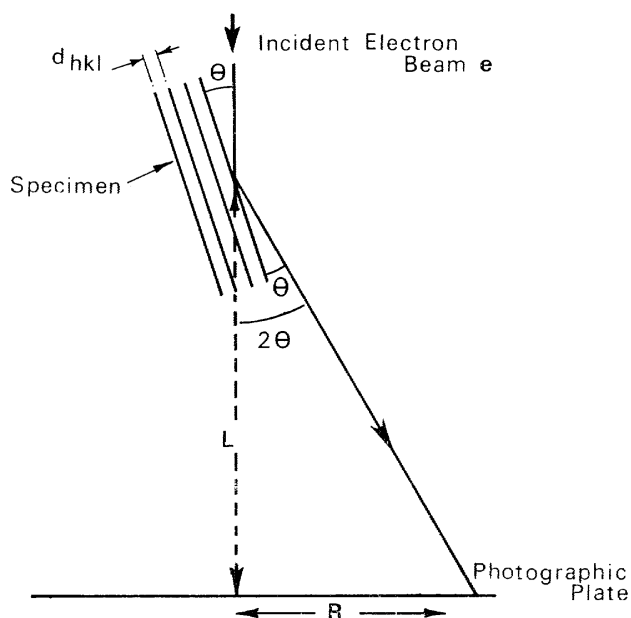


Fig. I.153. The electron microscope considered as a simple electron diffraction camera. (From Beeston, 1973, p.224)

From Fig. I.153 it is seen that: $R/L = \tan 2\theta$

where R = distance to spot or ring in pattern measured from the center (at the optic axis)
 L = camera length

Since, for small θ , $\tan 2\theta = 2\theta = \sin 2\theta$, (Note: θ expressed in radians)

$$R = 2L\theta,$$

and, from Bragg's law for small θ , $2\theta = \frac{n\lambda}{d}$

$$\text{thus, } d = \frac{n\lambda L}{R}$$

c. Calibration of camera length, L

If the geometry of the system and wavelength of the electron beam are known exactly, the instrument constant, L , can be derived and spacings in the specimen can be calculated from measurements of R for spots or rings in the diffraction pattern. It is difficult to determine the wavelength accurately by experiment (and it may change with time) and it is impractical to measure the high voltage with sufficient accuracy to find the wavelength by calculation. The only practical method is to calibrate the instrument through the use of a diffracting substance of known

structure. Since the instrument constant depends on lens currents and object position, ideally the calibration pattern should be taken at the same time as the unknown specimen. For non-biological specimens, this is conveniently accomplished by evaporating the calibration substance on the grid before or after depositing the unknown substance. For biological specimens it may be useful to add a standard such as thin platelet crystals of catalase (Fig. I.124).

The calibration is accomplished by taking a diffraction pattern of a specimen whose d values are known, measuring the radial distances of the spots produced by the diffracted beam of, for example, orders 1, 2, and 3 for a number of known d values and then preparing a graph of distance R versus interplanar spacing, d . Evaporated films of gold, magnesium oxide, and thallium chloride make excellent calibrating substances since they have d values accurately determined by X-ray diffraction.

d. Producing the diffraction pattern

The diffracted beams are brought to a focus in the back focal plane of the objective lens (Fig. I.154). In normal (*i.e.* bright field) magnification mode of TEM operation, the intermediate image formed by the objective lens is the object plane for the first (intermediate) projector lens. If the strength of this projector lens is so weakened that the object plane of this lens coincides with the back focal plane of the objective lens, then the diffraction pattern will be imaged by the first projector and subsequently enlarged by further projector lenses (Fig. I.155).

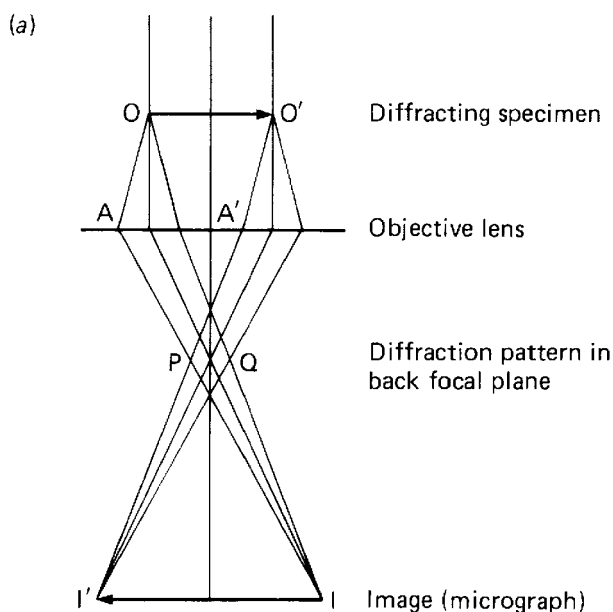


Fig. I.154. Ray diagram showing the formation of the diffraction pattern and intermediate image by the objective lens. Electrons diffracted in the same directions OA, O'A' come together to form a spot P in the back focal plane of the lens. Similarly, the diffraction spot Q is formed by electrons diffracted at an equal angle on the opposite side of the undeviated beam. (From Watt, 1985, p.122)

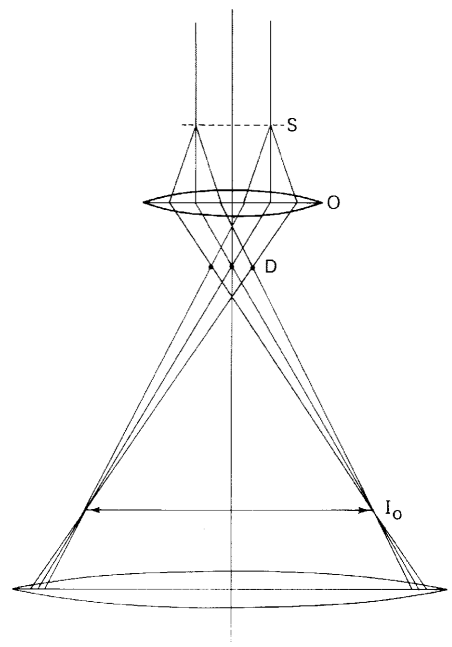


Fig. I.155. Formation of the diffraction pattern (D) and the intermediate image (I_0) of a crystalline specimen (S) by the objective lens (O). The intermediate lens (I) can be used to image either the intermediate image or the diffraction pattern. (From Agar, 1974, p.111)

The image plane and diffraction pattern both contain information about the specimen, but presented in different ways. Also, both are always present, to be viewed at will by selection of the strength of the intermediate lens. For optimum results (conditions for constructive interference that give rise to a sharp diffraction pattern) the specimen must be illuminated with a monochromatic, well-collimated beam (*i.e.* ideally a parallel beam but, in practice one that is nearly parallel with a very small aperture of illumination) to get good coherence. Under these conditions, all electrons striking a given spot on the specimen arrive from the approximate same direction. The objective aperture is usually withdrawn while recording the pattern; otherwise part of the pattern

may be cut off. Recall that the objective aperture and the primary electron diffraction pattern are both located in the back focal plane of the objective lens.

Selected area diffraction (Figs. I.156-I.160)

Insertion of an aperture in the **image** plane of the objective lens is effectively "equivalent" to placing an aperture in the plane of the specimen, but one that is smaller by a factor equal to the magnification of the objective lens (often 30-50 times). Thus, an aperture of diameter $50\ \mu\text{m}$ in the intermediate image plane can be used to define a $1\text{-}\mu\text{m}$ diameter region at the specimen. This region is then the one giving rise to the diffraction pattern transmitted by the selector aperture.

The selected area diffraction, or SAD, technique cannot be used to define regions much smaller than $1\ \mu\text{m}$ diameter because the spherical aberration of the objective lens causes some widely scattered electrons to be included in the recorded pattern even when they do not arise from the selected region.

A disadvantage of the SAD method is that, with a three lens imaging system with a fixed focal length projector lens, the objective lens must project an intermediate image precisely into the selector aperture plane and this means there is only one magnification at which the diffraction pattern can be viewed. Microscopes with four-lens imaging systems have the additional degree of freedom that the second intermediate lens (the first intermediate lens is normally called the diffraction lens) can be varied without restriction to give a wide range of camera lengths.

An alternative procedure is to select small areas in the specimen directly using a double condenser lens system to reduce the size of the area illuminated. Unless C1 is strongly excited to give a small illuminating beam, the beam will be incoherent and spots in the diffraction pattern will be broad and diffuse (Fig. I.160). With C1 strongly excited, the illumination beam will be small and highly coherent but very weak, necessitating long exposure times (sometimes minutes) to record the diffraction patterns.

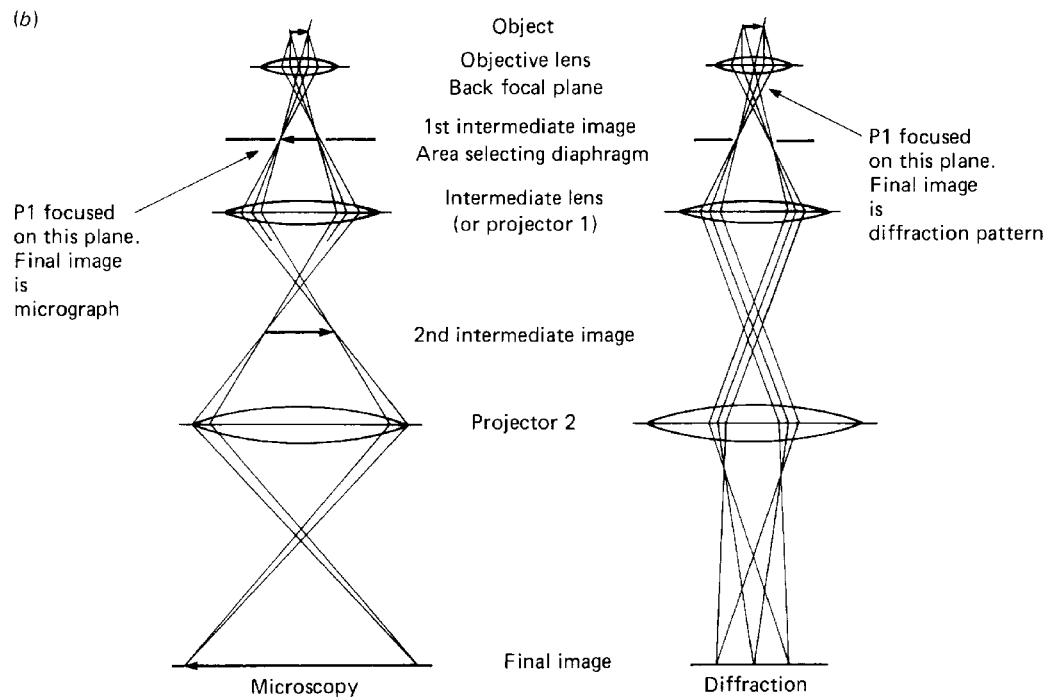


Fig. I.156. In a three-lens microscope the intermediate lens (or Projector 1) is normally focused on the intermediate image formed by the objective lens. When P1 is weakened to focus on the back focal plane of the objective lens, the final image is an enlarged diffraction pattern. The selected-area diaphragm ensures that only electrons coming from a chosen region in the specimen contribute to the diffraction pattern. (From Watt, 1985, p.122)

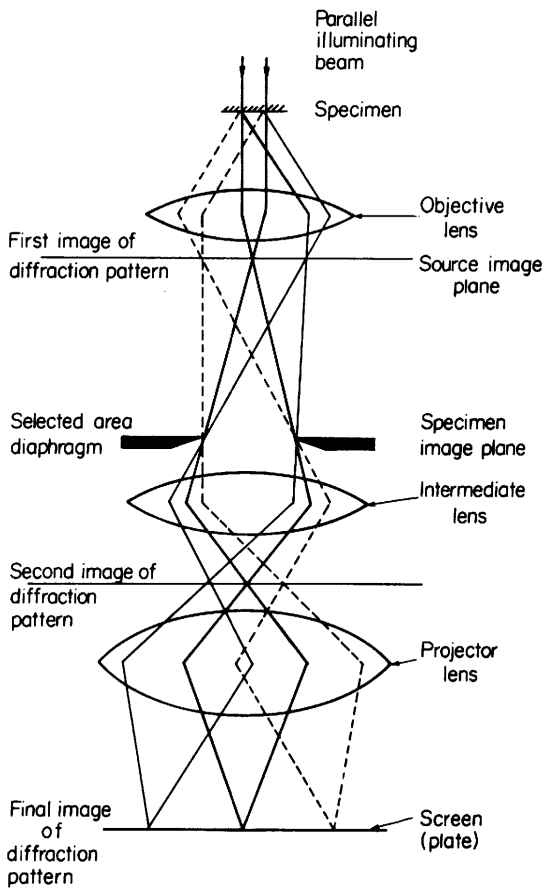


Fig. I.157. Ray diagram for selected area diffraction. The specimen is illuminated with as nearly parallel a beam of electrons as possible. The objective lens forms an image of the diffraction pattern at its back focal plane (the objective aperture diaphragm, which normally intercepts this pattern, must be withdrawn). An image of the specimen will be formed in the lower conjugate plane, so that a diaphragm placed in this lower plane will also be in focus with the specimen. This primary image is enlarged by the objective, so that a relatively large diaphragm will intercept all but the rays from a very small area of the specimen. The intermediate lens strength is now adjusted so as to form an image of the diffraction pattern from this selected area in the upper conjugate plane of the projector lens, which in turn forms a magnified image of the diffraction pattern on the screen or plate. (From Meek, 1970, p.287)

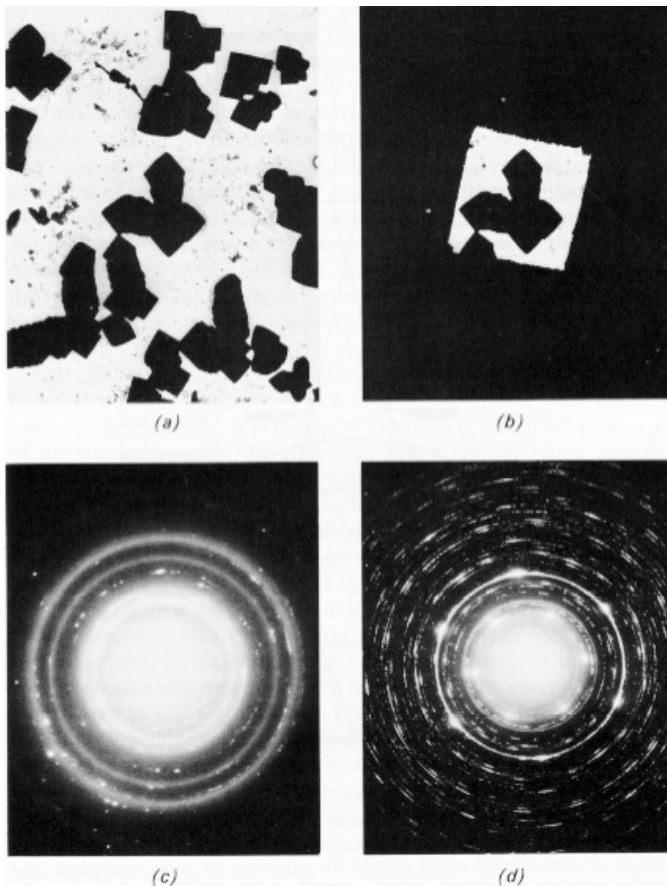


Fig. I.158. Obtaining a SAD pattern. (a) A suitable area of specimen including obviously crystalline material is found. (b) A small area is selected by suitably manipulating the four area selection blades (or by inserting a diffraction aperture of suitable diameter). (c) The source is focused on the screen with the intermediate (diffraction) lens, the condenser is defocused fully and the objective aperture is withdrawn. The pattern of dots and circles is the diffraction pattern of the specimen. The sharply-defined pattern (d) is of unsupported aluminum oxide. The poor definition of (c) is due to the thickness of the specimen (sodium chloride crystals) and the presence of the carbon and Araldite supporting films. (From Meek, 1970, p.288)

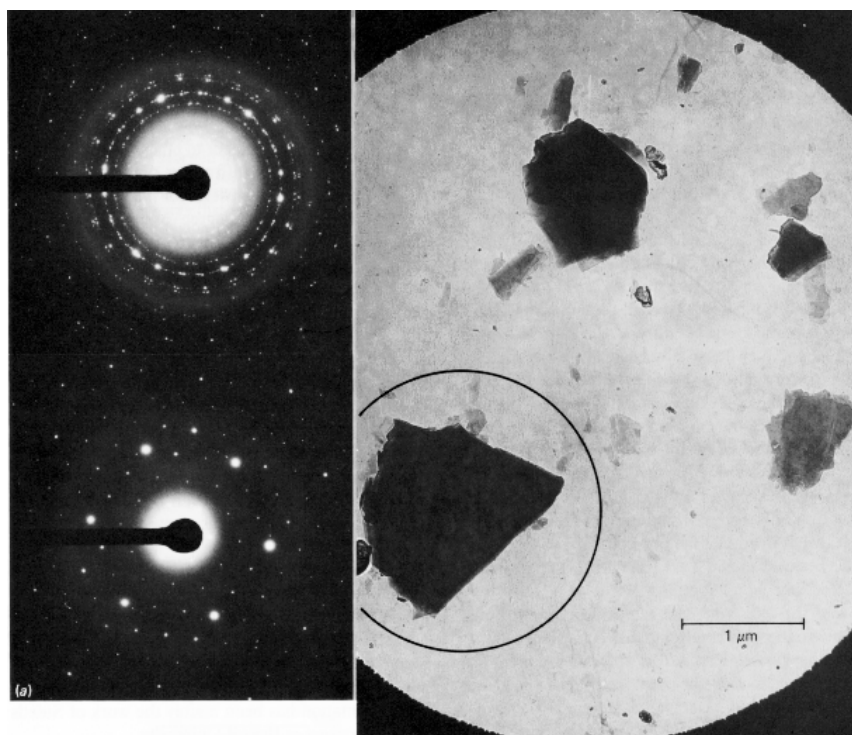


Fig. I.159. SAD patterns from selected small areas. The micrograph shows a field of crystalline particles outlined by a large selection aperture (corresponds to $\sim 6 \mu\text{m}$ at the specimen). The resultant 'spotty ring' type of diffraction pattern (upper left) indicates that the crystals are oriented in a number of different directions. Using a smaller selecting aperture ($2.3 \mu\text{m}$ at the specimen) positioned as indicated, the pattern is formed from the chosen crystal alone, giving the single-crystal pattern seen at lower left. (From Watt, 1985, p.124)

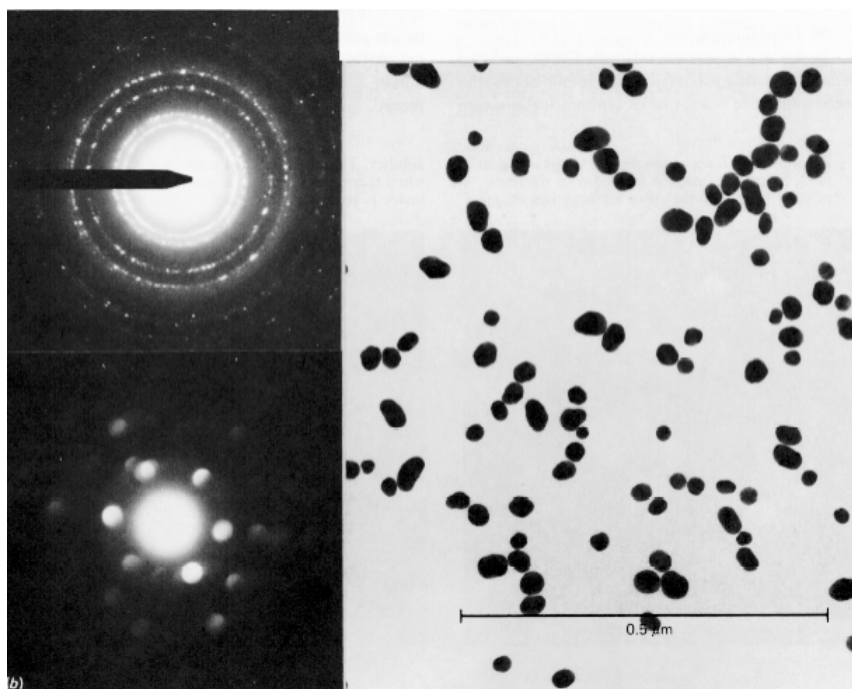


Fig. I.160. SAD micro-diffraction. The patterns and explanation are similar to Fig. I.159 but the field of view is less than $1 \mu\text{m}$ across and hence too small for conventional SAD. A single particle has been selected for diffraction analysis by focusing the illumination into a spot covering the particle. The diffraction spots are discs rather than points because the electron beam is no longer parallel at the specimen, but in the shape of a cone; each diffracted beam is therefore also a cone, which becomes a disc in the film plane. Discs can overlap and obscure others; hence, analysis of smaller crystals from μ -diffraction patterns is less precise than conventional SAD. (From Watt, 1985, p.125)

Converging beam method

In this method all the imaging lenses (O, D, I, and P) are turned off and the Fresnel diffraction pattern is observed (Fig. I.161). This pattern is approximately equivalent to the Fraunhofer pattern (the diffraction pattern that forms at infinite screen distance) since the distance of the final viewing screen from the specimen ($500\text{-}1000 \text{ mm}$) is large relative to the size of the specimen ($1\text{-}10 \mu\text{m}$) and spacings ($0.1\text{-}10 \text{ nm}$) that give rise to the pattern.

The advantage in operating in diffraction mode without lenses between the specimen and final viewing screen is the avoidance of lens aberrations and dependence of calibration on focal lengths

and object position. With a double condenser, the source is focused by C_2 on the final screen. The camera has a simple geometry and good length. The main disadvantage of the method is that the area illuminated at the specimen is about the size of the condenser aperture (usually $100\mu\text{m}$) and one cannot select small areas. This method is therefore of little use to biologists.

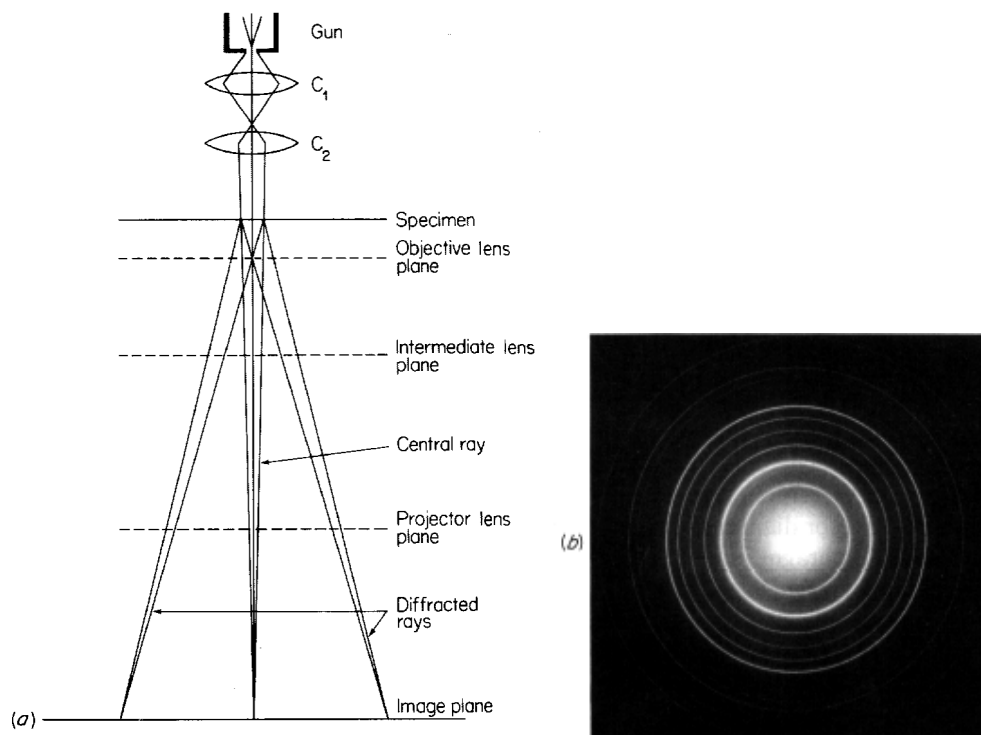


Fig. I.161. Electron diffraction without the use of image-forming lenses. The double condenser illuminates a selected area of the specimen, and the scattered pencils are focused on the screen by the action of condenser lens 2, C_2 . The resulting diffraction pattern (b) is an image of the electron source after interference with the specimen. The method is only of use for very close (interatomic) spacings; the diffraction pattern is normally enlarged by the action of the image-forming lenses. (From Meek, 1970, p.285)

Low angle electron diffraction

The conventional electron diffraction mode is useful for examining information on structures with spacings up to a few tenths of a nanometer ($<0.4\text{nm}$). For larger structure spacings such as are present in most biological macromolecules, the diffracted information is scattered through very small angles and tends to be lost in the intense central spot from the unscattered and inelastically scattered electrons.

The objective lens may be switched off, and the electron beam focused by the second condenser lens on the object plane of the intermediate lens (Fig. I.161). Alternatively, the objective lens strength can be reduced to increase its focal length so its back focal plane lies closer to the projector system and, consequently, a larger magnification of the final diffraction image results.

This is a powerful method because the recording of X-ray diffraction patterns from such specimens would be exceedingly difficult.

e. Advantages of electron diffraction

- Very small specimen areas can be studied, thereby allowing specific crystalline regions to be isolated and characterized.
- Translational vibrations or unidirectional drift of the specimen does **not** affect diffraction patterns since each bundle of parallel diffracted rays is still brought to focus in the same position in the back focal plane of the objective lens regardless of the translational position of the specimen. However, rotation of the specimen causes the diffraction pattern to rotate in the same direction, leading to smearing of the recorded pattern.

I.F.2. Dark Field Microscopy

A **bright field image** in electron microscopy is formed when the unscattered electrons of the incident beam combine with the scattered electrons as modified by passage through the objective aperture. Dark areas in the image arise from specimen regions that scatter electrons widely and are stopped by the objective aperture. If the unscattered electrons are removed, the image is formed only from the scattered electrons (*i.e.* those which have interacted with the specimen) and a **dark field image** is produced. This imaging mode is called "dark-field" because the viewing screen is dark unless there is specimen present to scatter electrons. Dark field images typically have considerably higher contrast than bright field images although the intensity is greatly reduced, therefore requiring longer photographic exposures (Fig. I.162).

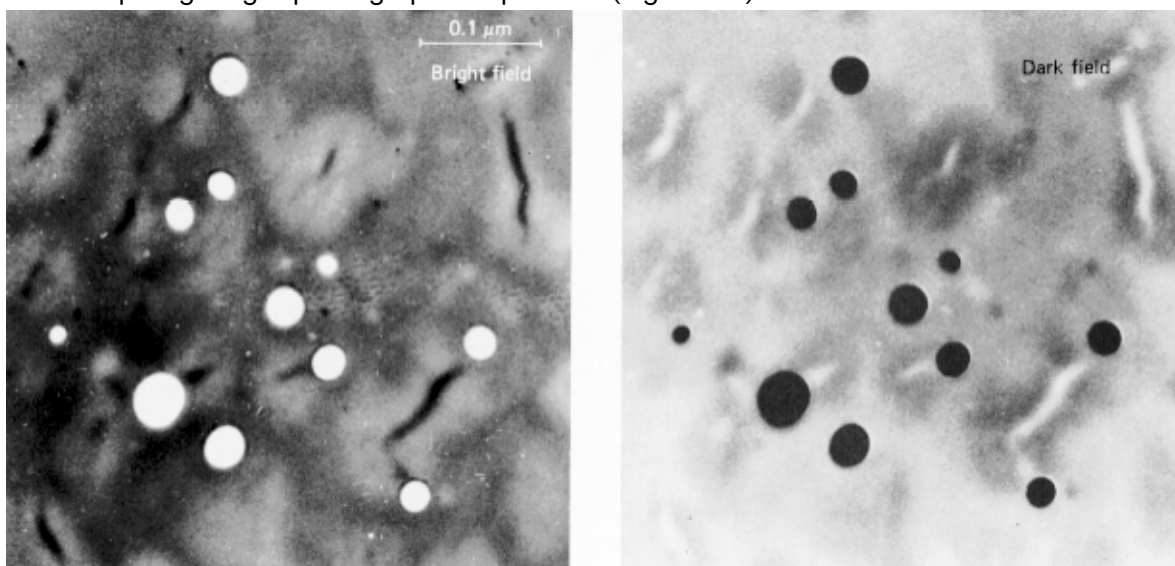


Fig. I.162. A holey carbon film in bright and dark field. Since one image is formed with electrons missing from the other, they are negatives of one another. The effect is most marked in the holes; when there is no electron scattering, the dark field image is completely black. (From Watt, 1985, p.126)

a. Methods of forming dark field images

There are several methods available for examining specimens using dark field microscopy.

Displacement of the objective aperture

The objective aperture can be displaced sideways to intercept the main unscattered electrons (Figs. I.163c, I.164a, and I.165a). This dark field image is of poor quality because the aperture accepts off-axis electrons subject to larger aberrations (spherical and chromatic) than those on the optic axis. The technique is useful for studying crystalline specimens where the aperture can be used to allow only certain diffraction spots/rings to be transmitted so only specific crystallographic orientations will be highlighted in the image.

Tilted illumination (High Resolution) mode

With the objective aperture kept in a symmetrical position on the optic axis, the incident electron beam is tilted at such an angle that it is intercepted by the aperture and the diffracted beam of interest travels down the objective lens axis and thus is subject only to the minimum aberrations suffered by a bright field image (Figs. I.163b, I.164b, and I.165b). Most modern microscopes include a convenient electrical tilting system for the electron beam that enables the operator to steer the incident beam in any required direction by a simple control. In order that this technique should operate smoothly and easily, it is essential that the tilt control should introduce only tilt of the beam without introducing lateral shift of the beam at the object plane. This method is particularly useful for studying crystalline specimens since the operator can follow the process of tilting the beam while in diffraction mode so the electrons in a particular diffraction spot can be made to pass down the axis of the electron microscope.

Strioscopic dark field

In this mode of dark field imaging the central, undeviated beam is stopped by either a physical stop on the objective aperture or by using an annular condenser aperture.

Beam stop aperture

The central beam stop aperture is a normal objective aperture with a fine wire welded across its center. This stops the undeviated beam and allows only the electrons scattered by the specimen to form the image (Fig. I.163d). This has been useful in high voltage microscopy (1000 kV) where contrast is very low. Details that may be nearly invisible in bright field appear in good contrast using this technique. A drawback is that, due to the asymmetry of the objective aperture, the astigmatism correction for the bright field does not hold in dark field. Since Fresnel fringes are absent in dark field (remember that Fresnel fringes are a consequence of phase contrast that arises from interference of the scattered electrons with the unscattered electrons) astigmatism correction in dark field is extremely difficult.

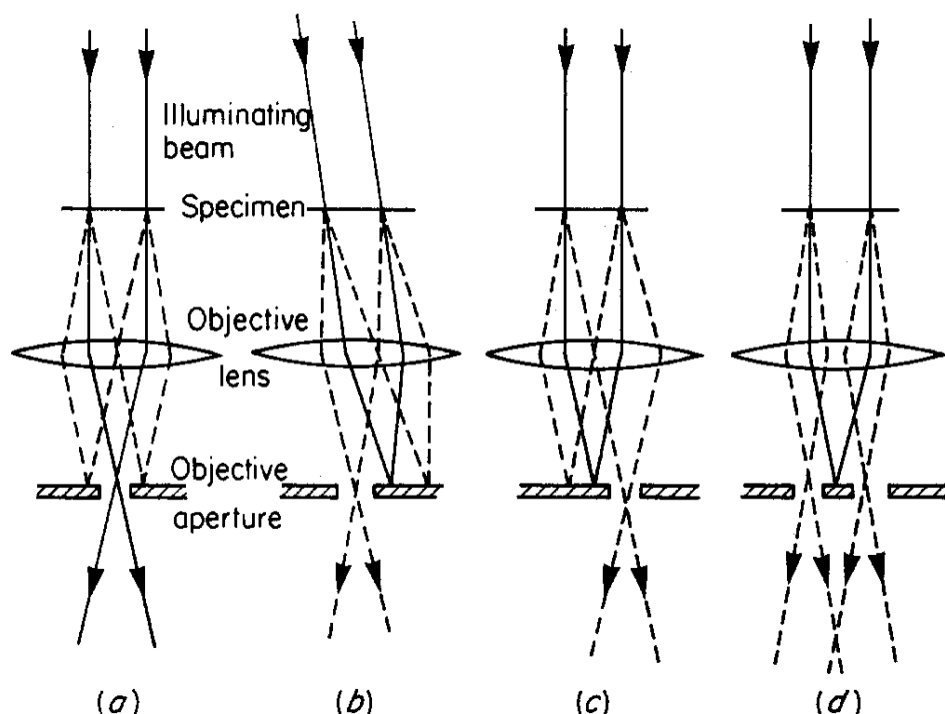


Fig. I.163. Methods for obtaining dark-field images. (a) Normal, bright-field TEM, in which the central pencil (full lines) passes through the objective aperture, but the objective aperture intercepts the scattered pencils (dotted lines). (b) Beam-tilt method. The illuminating beam is tilted so that the central objective aperture intercepts the direct pencil. One scattered pencil enters the imaging system. (c) Off-centered aperture method. The objective aperture is moved to one side so as to just intercept the direct pencil. The image is formed by the extreme peripheral scattered pencil, and is necessarily of low resolution owing to the increased effects of spherical aberration. (d) Beam-stop aperture ('contrast screen') method. A fine wire is placed across the center of the objective aperture, which intercepts the direct pencil. Almost all of the peripheral scattered pencils enter the imaging system, giving a brighter image than is obtained in (c). (From Meek, 1970, p.282)

Annular condenser aperture (Fig. I.166)

An annular condenser aperture can be used in place of the normal condenser aperture to produce dark field images. C2 is brought to a focus on the specimen, in which condition the illumination appears uniform over the specimen (when the condenser lens strength is altered, a hollow beam can be seen). In the absence of a specimen, the conical illumination forms a ring in the back focal plane of the objective lens. The unscattered electron beam falls onto the edge of the objective aperture and is prevented from reaching the image. The diameters of the objective aperture and annular condenser aperture must be carefully chosen so the hollow illuminating beam is correctly intercepted in the back focal plane of the objective lens. Any electrons scattered by the specimen that are able to pass through the objective aperture will form a high quality dark field image.

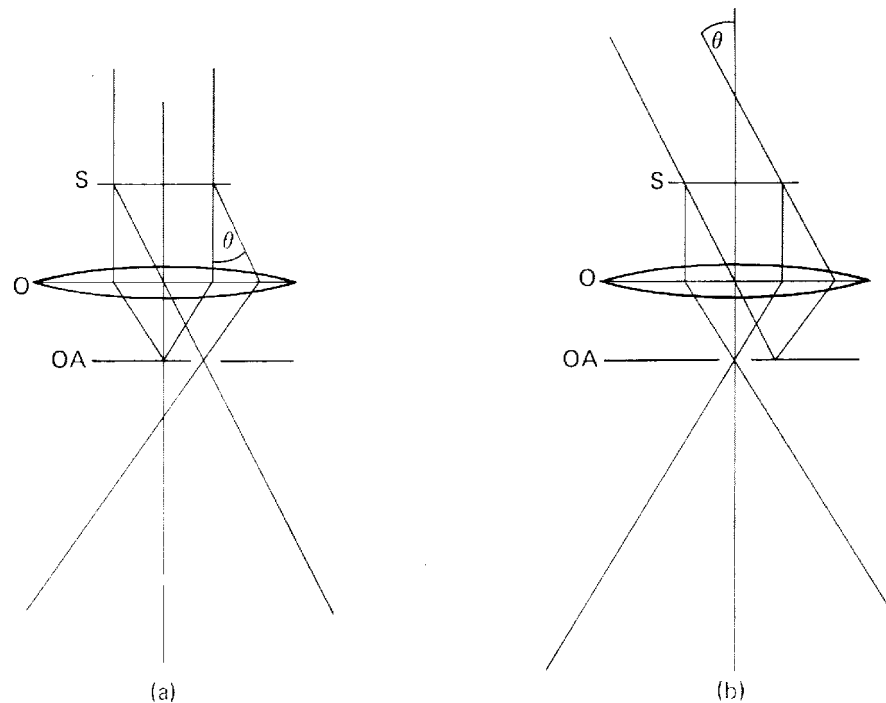


Fig. I.164. Formation of dark field images. (a) Normal illumination. The objective aperture (OA) is displaced from the axis of the objective lens (O) to accept the beam diffracted by the specimen (S) through the angle θ , and cuts off the unscattered beam. (b) The illuminating beam is tilted through an angle θ so that the diffracted beam passes down the axis and through the objective aperture (OA). (From Agar, 1974, p.115)

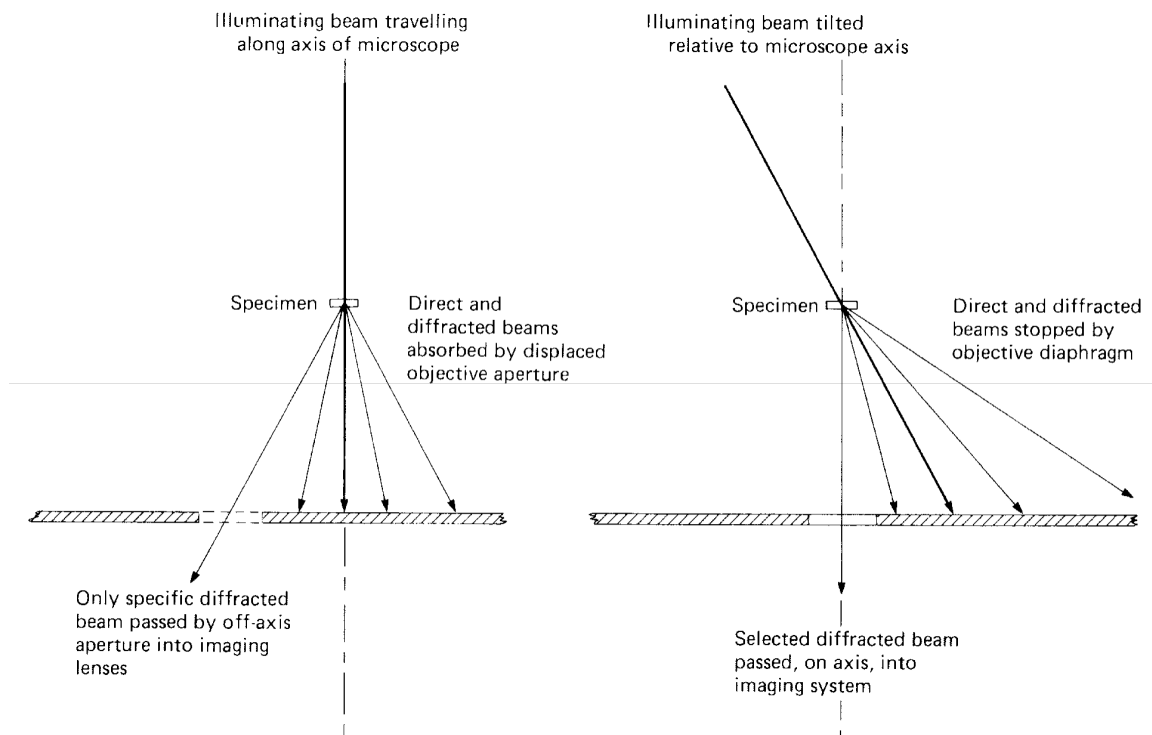


Fig. I.165. Dark field microscopy with the TEM. (a), (b) Schematic diagrams of two common methods of dark field imaging. (From Watt, 1985, p.127)

The advantage of this method over others is that it gives completely symmetrical illumination about the axis and consequently there is no danger of asymmetric charging of the objective aperture, and hence change of astigmatism. A normal aperture can be used to replace the annular condenser aperture to provide a bright field image for astigmatism correction, which will thereafter remain unchanged when the annular aperture is reintroduced. Because focused illumination is used in this method the specimen must withstand high irradiation and the magnification must be rather high so the beam uniformly fills the field of view.

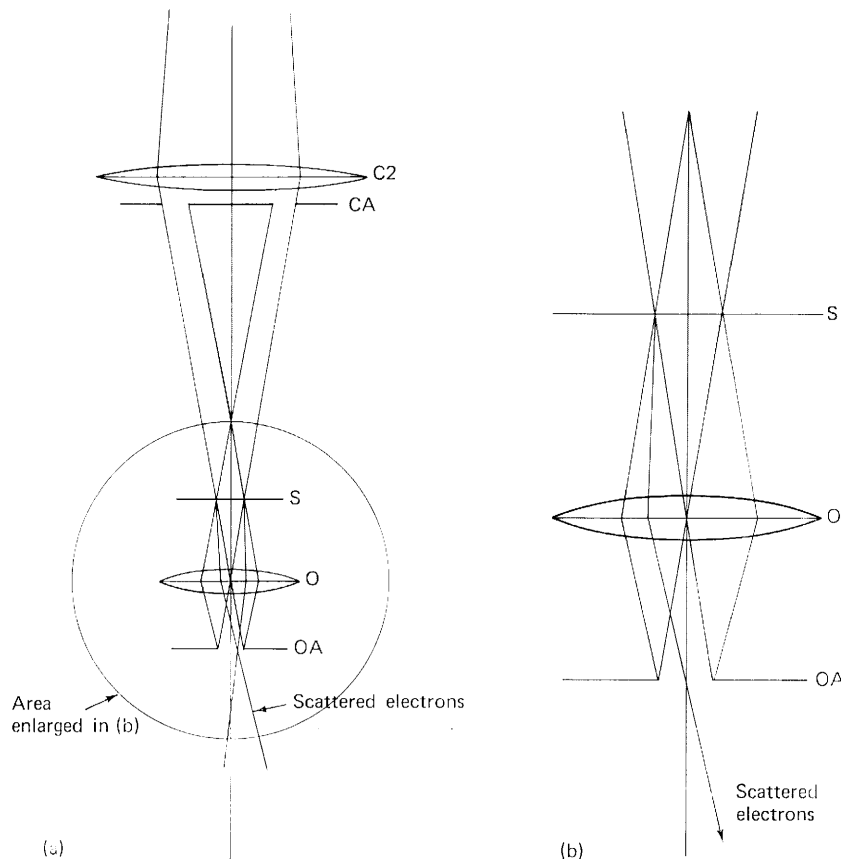


Fig. I.166. The annular aperture system for strioscopic dark field microscopy. (a) The annular condenser aperture (CA) forms a hollow illuminating beam, which illuminates the specimen (S) evenly when the second condenser lens (C2) is focused. Unscattered electrons are stopped on the edge of the objective aperture (OA), but electrons scattered by the specimen pass through the aperture. (b) Area of the objective lens enlarged to show the rays more clearly. (From Agar, 1974, p.119)

b. Advantages and disadvantages of the dark field technique:

Advantages

- Provides high contrast for examining molecules with very low contrast such as DNA (Fig. I.167).
- For crystalline objects, specific diffraction spots can be selected in the back focal plane of the objective lens in order to form a dark field image only from the electrons scattered by a chosen set of crystal planes.

Disadvantages

- More difficult to focus and correct for astigmatism since phase contrast is not present.
- Since the objective aperture transmits only a small fraction of the scattered beam, image brightness is low, necessitating longer exposure times to get usable photographic images. Consequently, specimens are subjected to greater levels of radiation damage.

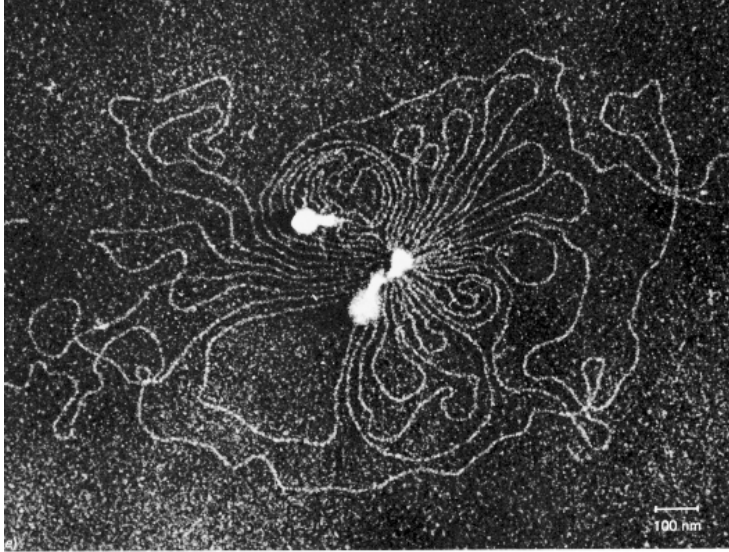


Fig. I.167. Strioscopic dark field micrograph (at 100 kV) of unshadowed and unstained filaments of DNA extracted from T4 bacteriophage by Kleinschmidt's method. (From Watt, 1985, p.130)

I.F.3. High Resolution Transmission Electron Microscopy

If the main objective is to resolve the finest possible detail in specially prepared specimens it is advantageous to use the shortest possible wavelength illumination (high voltage), an objective lens with very low aberrations, and a microscope with extremely high mechanical and electrical stabilities. Remember that high resolution requires BOTH high instrumental resolving power and high image contrast. High resolution cannot be achieved unless both of these factors are adequate. Since instrumental factors that favor image contrast tend to cause resolving power to deteriorate and vice versa, resolution may sometimes be improved in practice, by improving either resolving power or contrast at the expense of the other.

Some of the important considerations with regard to high-resolution imaging are briefly outlined in the sections that follow.

a. Shorter wavelength electrons (better diffraction limited resolution)

Commercial microscopes with 200-400 kV accelerating voltages are now becoming more routine (and even close to affordable) and there are a couple of microscopes of experimental design offering 1 MeV or even higher (Fig. I.168). Such very high voltage microscopes are extremely large (spanning at least two floors of a building) and must be mounted in special suspension systems to isolate them from site vibrations. The high voltage generators offer electronic stabilization to one part in 10^6 .

b. Reducing spherical aberration

Improvements in lens design are required to reduce image defects caused by spherical aberration. This requires increasing the magnetic field and thus reducing the focal length of the objective lens. Practical limitations such as the magnetic saturation of iron, which limits the flux density of the lens field using the conventional form of construction to about 25,000 gauss, make it impractical to achieve a focal length much less than 1 mm. The use of iron free lenses having superconducting coils cooled by liquid helium allows intense fields of 50,000 gauss to be generated. However, the rate of gain in resolving power falls off as the focal length decreases.

Another proposed method for reducing spherical aberration consists of using a "single-field condenser-objective" lens. This is a very powerful symmetrical lens with the specimen placed at the center of the bell-shaped field instead of a little above it, as is the case with the conventional type of objective lens. The upper pole piece acts as a condenser, focusing the incident beam on the specimen and the lower pole piece acts as an objective lens of short focal length. This type lens has about one-tenth the spherical aberration and one-half the chromatic aberration of the conventional lens.

Finally, another approach to reduce lens aberrations is to combine lenses as is done in light microscopy such that errors in one lens are compensated by those in subsequent lenses. It may be possible, for example to combine electrostatic negative lenses with electromagnetic positive lenses, although the practical difficulties are apparently very great. Another idea is to use a series of cylindrical electrostatic lenses in combination with round (symmetrical) electromagnetic lenses and correct for spherical aberration using computer control to calculate the necessary compensating signals for all the component lenses.

Recently, many scientists have been working to produce spherical aberration (Cs)-corrected electron microscopes using hexapole correctors (Haider *et al.*, 1998). The point resolution attained in a TEM using the image-forming Cs-corrector is reported to be better than 0.12 nm (Sawada *et al.*, 2005).

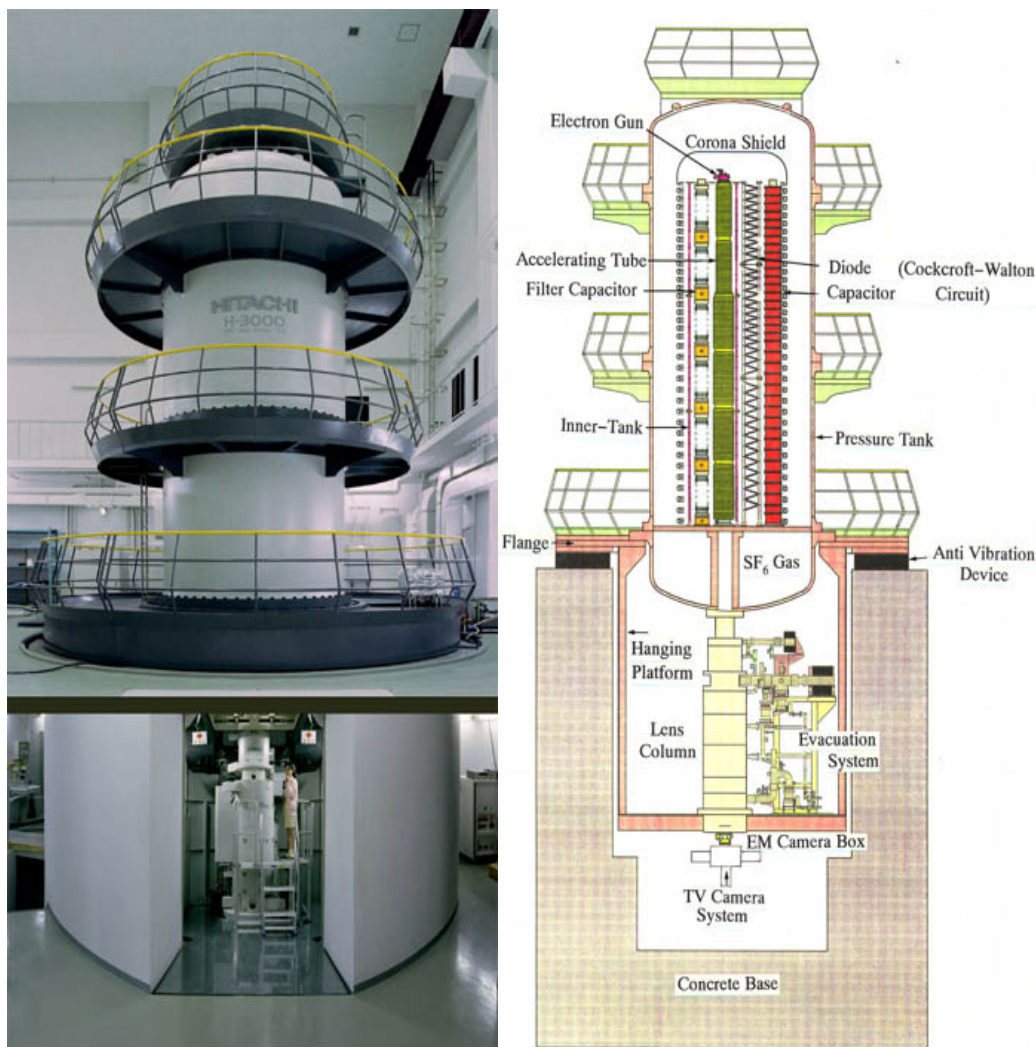


Fig. 1.168. The 3 million electron volt ultra-high voltage electron microscope (UHVEM) at Osaka University in Osaka, Japan.

c. Reducing chromatic aberration

Experiments with electron velocity filters, which work on the same principle as the mass spectrometer, have shown that it is possible to improve both resolution and contrast. After passing through the specimen, the beam becomes heterochromatic and passes through the objective lens in the usual way. In the **Castaing electron velocity filter**, a wedge-shaped magnetic field between the objective lens and the rest of the imaging system causes electrons of different speeds to follow different paths, so that they can be sorted out by causing them to fall on either side of a slit aperture. Electrons emerging from the slit are monochromatic and can be imaged by a conventional intermediate and projector system with greatly reduced chromatic

aberration in the final image.

d. Compensation for lens asymmetry

Realization of the full resolving power of an electron microscope is dependent upon compensation of lens asymmetry to a level consistent with that resolving power. Compensation to the level required for ultimate resolution is difficult to achieve or maintain, therefore lens asymmetry is the defect, which tends to limit resolution in practice. Some of the newest, computer-controlled microscopes now have the capability to perform lens astigmatism corrections and focusing operations under software control. Such technology provides for more reliable microscope operation and reduces some of the tedious and time-consuming operations performed by the microscopist.

e. Critical focusing

In general, the higher the target resolution, the more critical focusing becomes. Thus, although focusing poses no theoretical limit to resolution, it is so critical that difficulty in selecting focus is often a practical limitation on resolution. Fine focusing is aided by operation at high magnification and high intensity, and sometimes by the use of an image intensifier.

f. Alignment of the optical components

It should be obvious that there is no hope of achieving ultimate levels of resolution with a misaligned microscope.

g. Improvement of specimen contrast

As we will see in our discussions of specimen preparation, most methods that improve inherent specimen contrast do so at the expense of resolution. For example, resolution of stained structures is limited ultimately by the size of the stain molecules themselves (which is in the range 0.5-1.0 nm for stains used with biological specimens).

h. Use of more intense electron sources

The use of pointed filaments, LaB₆ cathodes, or field emission guns to produce a smaller, more intense illumination spot helps in at least three ways:

- Improved image interference contrast because the electron beam is more coherent
- Improved visibility during instrumental adjustments, which makes focusing and astigmatism compensation easier.
- Allows for reduced exposure times, thus reducing the effects of residual specimen drift or vibrations.

I.F.4. Tilting and Stereo Microscopy

An electron microscope compresses information from what is a three-dimensional (3D) object into a 2D (projection) image. **Stereoscopy** is the visualization of objects in three dimensions and is based on the fact that the observer's two eyes have different viewpoints and the brain processes the information from these two sensors to give a mental impression of length, breadth and depth. Because of our binocular vision, we are able to fuse the two images we see from slightly different viewpoints to obtain information about the third dimension (depth).

In stereoscopic photography a camera with two separate lenses (or the same camera used in two separated positions) is used to record a scene from two viewpoints; when the two views are presented to the observer so that each eye sees a different image he obtains the impression of seeing the scene in depth. The pair of photographs giving the two views of the same scene is termed a **stereoscopic pair**.

a. Tilting for interpretation

Stereo viewing can be an important technique for sorting out three-dimensional structures. For specimens of moderate thickness, the tilt angle required to obtain the stereo effect is normally less than 10° . High magnification and a high tilt angle only become necessary for imaging very thin objects in stereo. The angle of tilt chosen must take account of the approximate vertical separation of the structures to be examined, and the final magnification at which the stereo prints will be viewed.

Often, for example in thin sections, the specimen may be oriented in an unfavorable direction for viewing and it helps to be able to tilt the section to obtain a better view of the structure. For example, a section through a cellular membrane may cut through the membrane obliquely and it may be advantageous to tilt the section to obtain either an edge view or a face view of the membrane to aid in the interpretation of the membrane structure (Fig. I.169). It may be necessary to tilt the specimen through large angles ($>45^\circ$) since the direction of the structure may be quite random within the section. Typical goniometer tilt stages in modern microscopes allow specimens to be tilted up to at least $\pm 60^\circ$ or $\pm 70^\circ$, therefore it is possible to view some structures from two directions at right angles.

The use of a goniometer tilt stage also facilitates the examination of crystalline specimens where it is possible to orient the crystal with different crystallographic planes in the viewing direction.

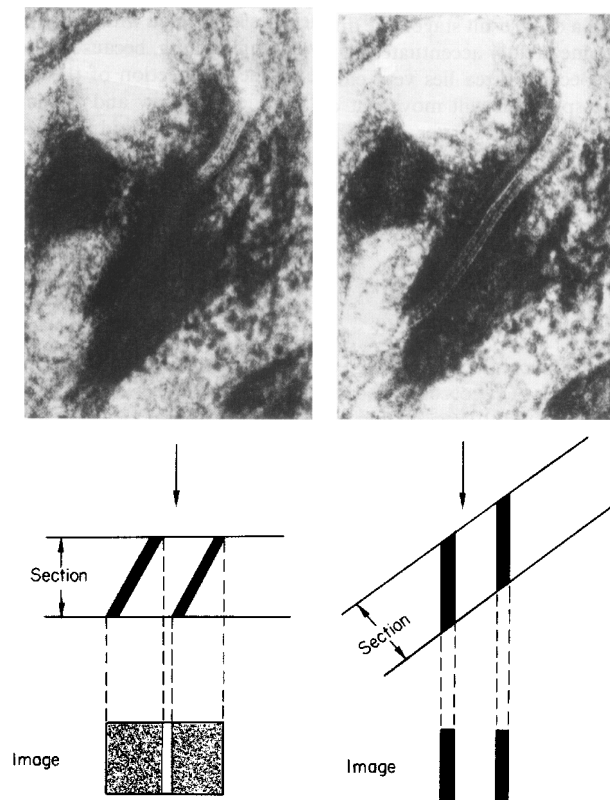


Fig. I.169. Advantage of a large-angle specimen double-tilt. Micrographs (top left and right) are of the same desmosome in a section of epidermis. The bright lines in (top right) are the membranous structure, invisible in (top left), which was taken with the specimen untilted in the microscope. The image of the membranes in (top left) is blurred due to object superposition as shown in (bottom left). When the specimen is tilted so as to bring the membranes parallel with the illuminating beam, as shown in (bottom right), the structure of the desmosome becomes clearly apparent in (top right). This method of investigating fine structure is also possible with single large-angle tilt plus 360° specimen rotation. (From Meek, 1970, p.291)

b. Stereo operation

To produce a stereo pair of images the specimen is first tilted through an angle on one side of the beam axis, and the required area is found, focused, and photographed. The specimen is then tilted

to the same angle on the other side of the beam axis, and the identical area is recentered, focused and photographed again. The two micrographs are then printed and the prints placed with their centers about 6-10 cm apart. The prints must be exactly parallel, set at the same vertical height and at the same magnification. They are viewed through a pair of narrow angle prisms with lenses arranged so as to converge the optical axes of the eyes inwards by about 15° (Fig. I.170). The images of the two members of the stereo pair are then superimposed and should fuse allowing the brain to interpret the 3D structure of the specimen. Experienced viewers can fuse the two images of a stereo pair without the use of any optical aid.

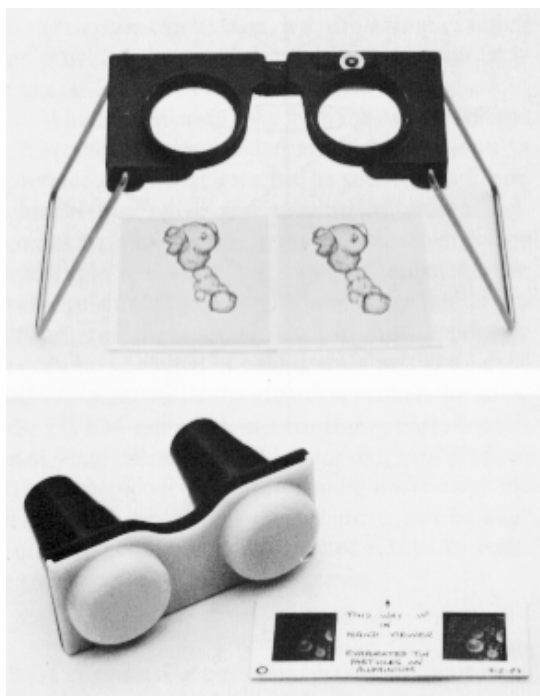


Fig. I.170. Simple viewers for stereoscopic pairs. 'Spectacles on stilts' enable a pair of prints up to 6.3 cm wide to be seen, enlarged, in 3D. The separation between the two halves of the viewer can be varied to accommodate differences in interocular separation between observers. The molded plastic transparency viewer accepts pairs of transparencies in 4.25 x 10.1 cm cardboard or metal frames. (From Watt, 1985, p.136)

Four parameters must be considered when making a successful stereo pair: θ , the full angle of tilt, P , the parallax, t , the specimen thickness and M , the overall viewing magnification (product of microscope, enlarger and stereo viewer magnifications). These are related by the following expression:

$$\sin(\phi/2) = \frac{P}{2tM}$$

Many TEMs are fitted with a stereo specimen holder giving a tilt angle of $\pm 6-7^\circ$ (the average angular separation between the eyes at a viewing distance of 25 cm). A magnification of 50,000X is approximately the highest magnification at which stereoscopic depth perception seems to work. At this small tilt angle a section thickness of at least $0.3 \mu\text{m}$ is required. As magnification is reduced, so specimen thickness must be increased. Thus, the stereo effect obtainable with the normal biological ultrathin section, even using a high angle tilt holder giving tilts of $\pm 60^\circ$, is barely perceptible.

Stereo is often useful for viewing shadowed surface replicas (Figs. I.171-I.173) because the replica itself is three-dimensional. The great depth of field of the transmission electron microscope ensures that the images are uniformly sharp throughout.

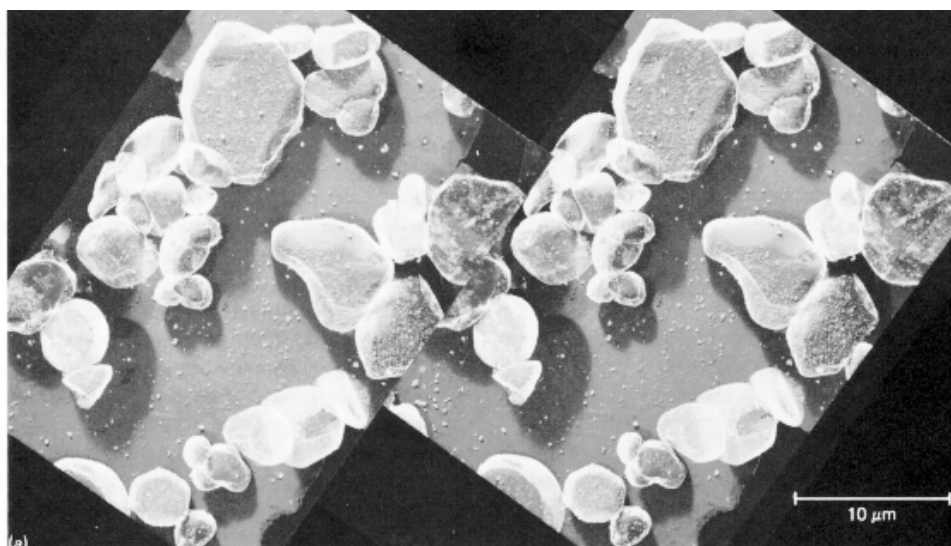


Fig. I.171. Stereoscopic pair of shadow cast replicas of surface-treated phosphor particles, taken with a specimen tilt of 9° . (From Watt, 1985, p.138)



Fig. I.172. Stereoscopic pair of shadow cast, two-stage replica of a diamond-ground glass surface. (From Watt, 1985, p.138)

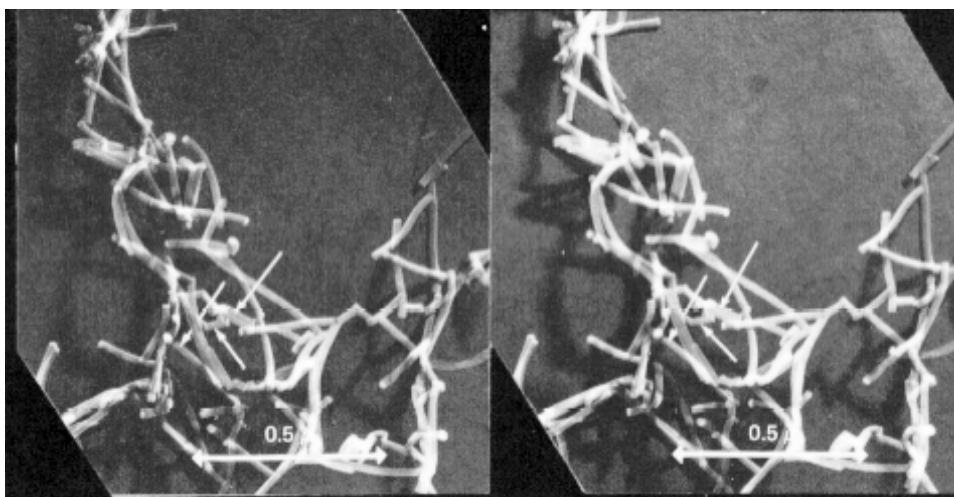


Fig. I.173. Stereoscopic pair of transmission micrographs of freeze-dried tobacco mosaic virus particles showing protein subunits. (From Watt, 1985, p.157)

c. Eucentric tilt stage

Unless the specimen area being imaged lies exactly on the electron optical axis and on the exact axis of tilt (exact center of the grid) it will move up and down with respect to the objective lens object plane while being tilted. The objective must then be refocused after tilting, which causes the image to slightly change magnification and rotate. Thus, it may be impossible to fuse the resulting pair of micrographs unless the enlarger magnification and print angle are changed to compensate for these errors during printing. In addition, if the object lies away from the center of the grid, the image will move out of the field of view while being tilted, and it must be kept centered on the screen with the stage controls. These disadvantages are overcome with the use of a **eucentric tilting stage** (Figs. I.174 and I.175) in which the axis of tilt can be adjusted to always intersect the electron optical axis.

Because the angular rotation of the image depends on the magnification (recall that electrons rotate as they pass through the lenses) the direction of the tilt axis in the specimen plane may have no simple relationship to the corresponding direction in the image plane. Unless the stereo pair of micrographs is oriented correctly, the stereo effect will be a reduced, or there will be no effect if the tilt axis in the image plane happens to lie along the line joining similar points in the two prints.

The stereo pairs must be observed under a stereo viewer and rotated about their centers until the direction of maximum 3D effect is reached or the microscope should be calibrated for each magnification so the necessary angular reorientation of the micrographs is known (e.g. Figs. I.171-I.173).

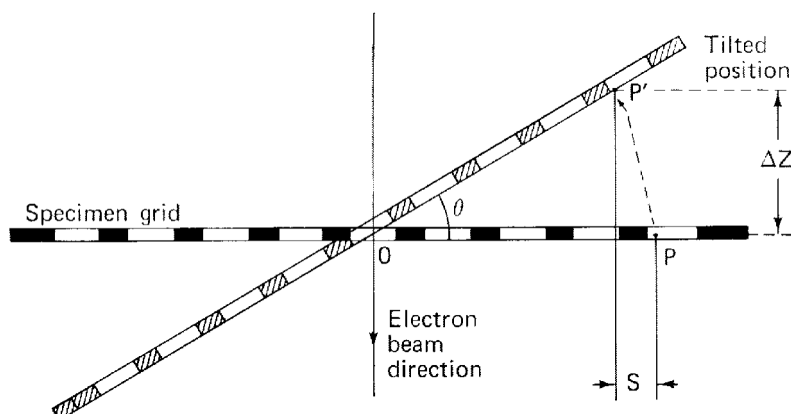


Fig. I.174. Effect of tilt of the specimen on the point of observation and the focal plane. For a tilt θ the point P moves laterally a distance S and the focal plane moves ΔZ . Note that the effect increases with the distance OP. (From Agar, 1974, p.56)

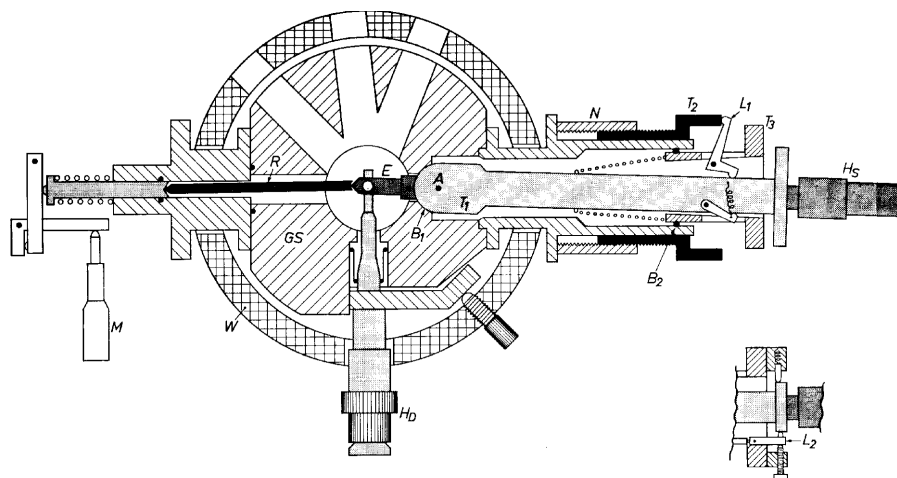


Fig. I.175. Top view diagram of the eucentric stage designed for older Philips electron microscopes. (From Agar, 1974, p.57)

d. Tilting to obtain 3D structural information

To completely determine the 3D structure of an asymmetric object, it is necessary to record several views (ideally covering a full 180° of views). The more closely-spaced the views, the higher the theoretical resolution that can be obtained. The use of high tilt goniometer tilt stages in modern microscopes makes it feasible to record tilt (tomographic) series from specimens in an angular range from -60° to $+60^\circ$ and sometimes -70° to $+70^\circ$. The use of tomographic image processing techniques is suitably designed to allow the reconstruction of 3D structures from the series of electron micrographs. This is discussed in greater detail in § III.

I.F.5. Low Temperature

One of the main reasons for studying specimens at low temperature is to reduce the effects of radiation damage since presumably the larger molecular fragments produced by radiation damage might not have sufficient thermal energy to move from their original locations. Reduction of radiation damage by as much as 5-10 times over that at room temperature has been found for some specimens at liquid helium temperature (4 K). In addition, the study of the native structure of biological specimens has been made possible by frozen-hydrated techniques where the specimen is quickly frozen in aqueous solution or *in vivo* and viewed in the microscope at near liquid nitrogen ($\sim 100^\circ\text{K}$) or liquid helium ($\sim 4\text{ K}$) temperatures. These topics will be dealt with in more detail during discussions on unstained specimens (§ II.A.5) and radiation effects (§ II.B).

I.F.6. Energy Loss

When an electron beam traverses a specimen in the TEM, for every characteristic K-shell X-ray photon generated, there will be an electron that has lost the characteristic energy $E_{K\alpha b}$ (Fig. I.176). By measuring the energy losses through a localized region of the specimen it is possible to infer the specimen composition.

Energy loss spectroscopy is a technique confined to relatively thin TEM specimens and is most usefully applied to light elements (*e.g.* sodium and below). Only a limited number of microscopes are equipped to carry out electron energy loss spectroscopy (EELS). "Thin" means thin enough for electrons to suffer only one inelastic collision. This is about 30-50 nm for biological material viewed with 100 kV electrons.

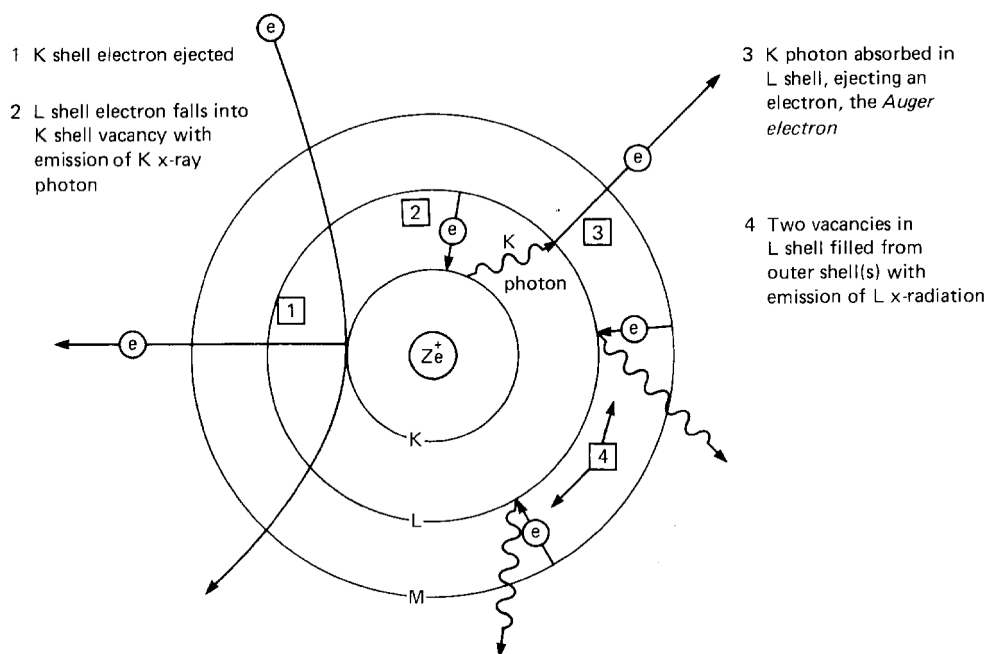


Fig. I.176. Schematic diagram illustrates the sequence of processes involved in the emission of Auger electrons. The transition illustrated would be identified as KLL, these being the shells involved in steps 1, 2, and 3 of the process. Other transitions are possible. (From Watt, 1985, p.274)

An energy analyzer, fitted at the bottom of the TEM column below the viewing screen, produces a spectrum of the energy distribution in the transmitted electrons relative to the primary beam energy (Fig. I.177). Most electrons in a spectrum are found in the initial **zero loss peak** and in loss peaks involving interactions with valence or conduction electrons, up to about 50 eV loss. Beyond this a smoothly falling background has superimposed on it the ionization edges of atoms whose X-ray absorption energies are reached. These are the peaks used for analysis.

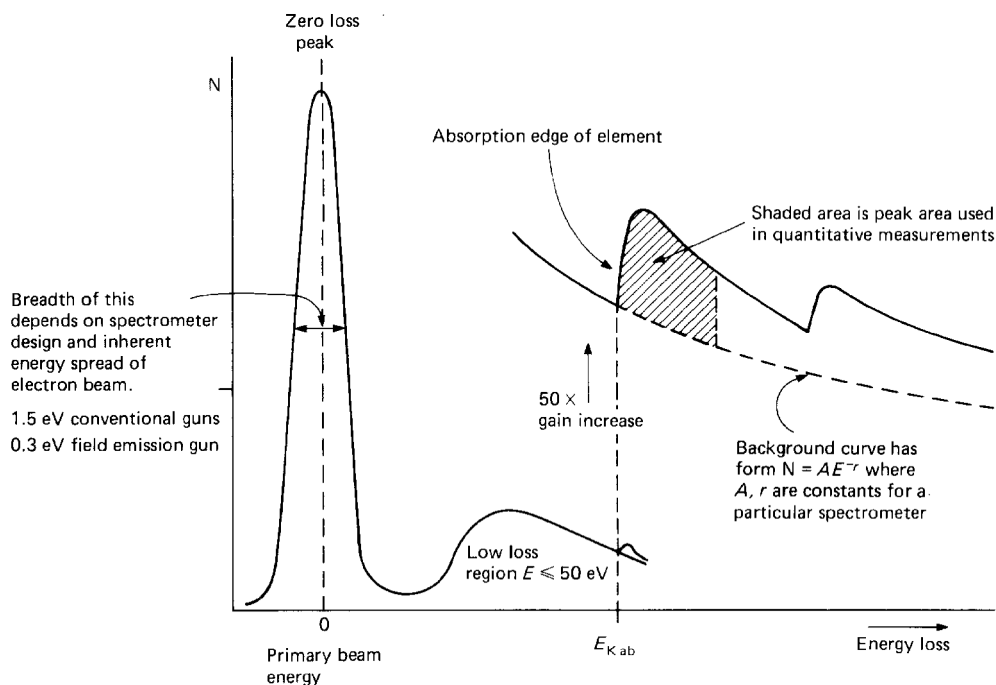


Fig. I.177. Characteristic form of an EELS spectrum. (From Watt, 1985, p.275)

Information on chemical bonding, molecular structure and dielectric constant may be obtained from a detailed study of energy loss curves. The resolution of fine structure depends on the design of the spectrophotometer and on the energy spread of the primary electron beam. This is wider (1.5 eV) from a thermionic tungsten filament than from a cold field emitter such as a field emission gun (0.3 eV).

I.F.7. X-Ray Microanalysis

When high velocity electrons interact with matter, electromagnetic radiation (X-rays and visible light) is also emitted (Fig. I.178). There are two sources of electron-induced electromagnetic radiation. The first is due to loss of energy from the incident electron to the outermost electron shells of the specimen atoms as it is slowed down during its passage through the specimen. This reappears as quanta of soft X-radiation. Since the slowing process is continuous and not stepwise, a continuous or 'white' spectrum of soft X-rays is emitted. The wavelengths of the emitted X-rays are between 10-100 nm.

As the energy of the incident electrons increases above 1 kV they are able to interact with the inner shells of specimen atoms. This causes an orbital electron to jump from a lower energy level shell to a higher energy shell. When it drops back, a quantum of energy in the form of a 'hard' or short-wavelength X-ray is emitted. Electron transitions from one shell to another involve very precise energy quanta, so the emitted X-ray is of a very precise wavelength or energy. Because the transition energies differ for each individual atomic species, the emitted wavelengths are characteristic of the atoms forming the specimen. By measuring the wavelength or energy of each of the emitted X-rays with an X-ray spectrometer, a qualitative analysis of the atoms composing the specimen may be made. If the relative intensity of the particular X-ray corresponding to a particular atomic species is measured, a quantitative analysis of the specimen may also be made.

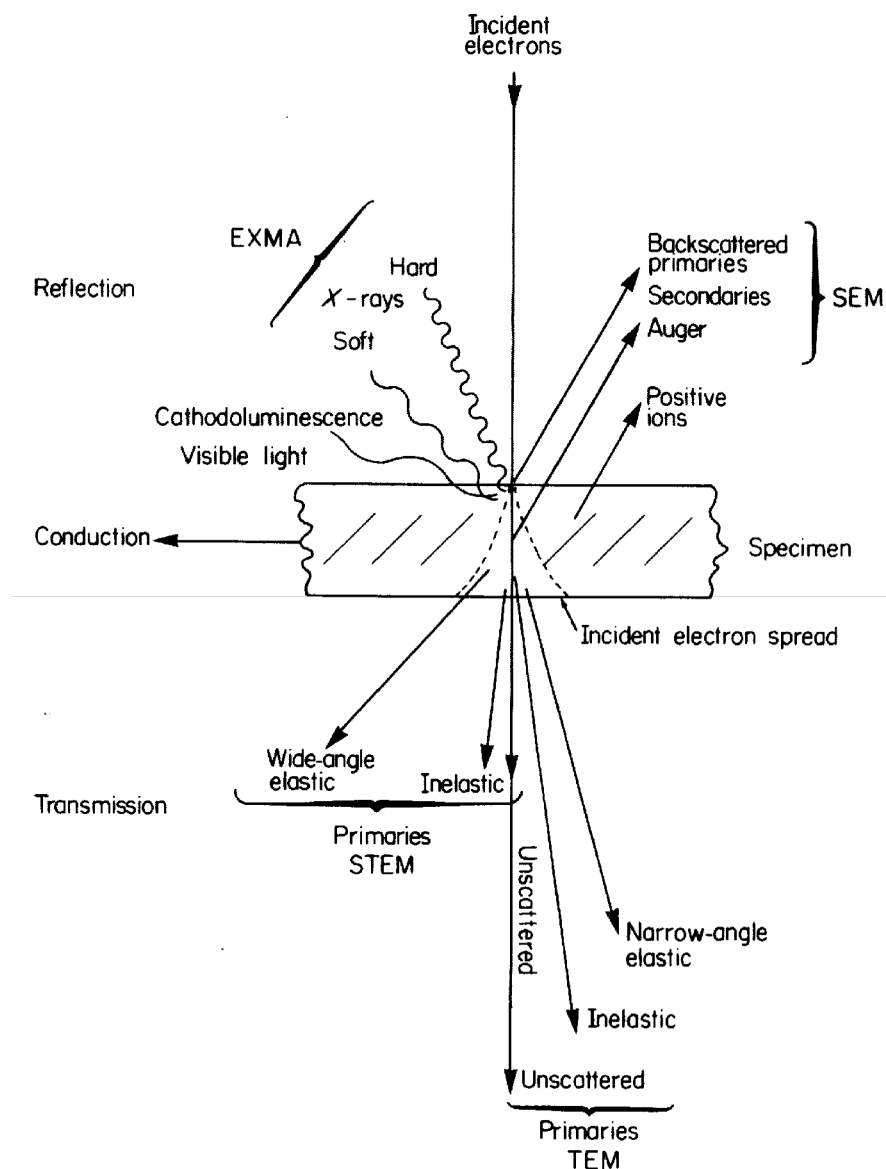


Fig I.178. Diagram shows the most important forms of interaction between a beam of high-energy incident electrons and the specimen. (From Meek, 1976, p.61)

The electron micro-probe X-ray microanalyser (EXMA) can be operated in either the probe mode or the scan mode. In the **probe mode**, the X-ray spectrum from a comparatively small volume of the specimen may be analyzed qualitatively for all the detectable elements present. In the **scan mode** the detector is set to an X-ray spectral line or an energy corresponding to a selected element, and the probe beam is scanned in a raster across the desired area of the specimen. A 'map' of the specimen in the 'light' of the selected element is generated on a synchronous display tube and recorded photographically. The electron gun is then set to give a wide-angle flood beam, and the conventional TEM image is focused on the final screen and photographed in the usual way. The two photographs can subsequently be superimposed to show the distribution of the selected element.

The **limits of detection** for analyzing elements from sodium to uranium from a region of 100-200 nm diameter, range between 10^{-14} and 10^{-19} gm. The low X-ray yield makes the low-Z elements of biological significance very difficult to detect and quantitate. Due principally to the lateral spread of the electron probe as it passes through the specimen, X-rays are generated from a greater volume of the specimen than would be expected simply from consideration of probe spot size.

I.F.8. References Cited in §I.F.

- Agar, A. W., R. H. Alderson, and D. Chescoe (1974) Principles and Practice of Electron Microscope Operation, pp. 1-345. *In* A. M. Glauert, Ed., Practical Methods in Electron Microscopy. Vol. 2, North-Holland Pub. Co., Amsterdam.
- Beeston, B. E. P. (1973) An introduction to electron diffraction, pp. 193-323, *In* A. M. Glauert, Ed., Practical Methods in Electron Microscopy. Vol. 1, North-Holland Pub. Co., Amsterdam.
- Blundell, T. L., and L. N. Johnson (1976) Protein Crystallography, p. 565, Academic Press, N. Y.
- Haider, M., H. Rose, S. Uhlemann, E. Schwan, B. Kabius, and K. Urban (1998) A spherical-aberration-corrected 200 kV transmission electron microscope. *Ultramicrosc.* **75:53-60**.
- Meek, G. A. (1970) Practical Electron Microscopy for Biologists, 1st Ed., p. 498, Wiley-Interscience, London.
- Meek, G. A. (1976) Practical Electron Microscopy for Biologists, 2nd Ed., p. 528, John Wiley & Sons, London.
- Sawada, H., T. Tomita, M. Naruse, T. Honda, P. Hambridge, P. Hartel, M. Haider, C. Hetherington, R. Doole, A. Kirkland, J. Hutchison, J. Titchmarsh, and D. Cockayne (2005) Experimental evaluation of a spherical aberration-corrected TEM and STEM. *J. Elec. Microsc.* **54:119-121**.
- Watt, I. M. (1985) The Principles and Practice of Electron Microscopy, 1st Ed., p. 303, Cambridge University Press, Cambridge.